

See discussions, stats, and author profiles for this publication at: <https://www.researchgate.net/publication/51456573>

# Theoretical Study on the Regioselectivity of the B-80 Buckyball in Electrophilic and Nucleophilic Reactions Using DFT-Based Reactivity Indices

ARTICLE in THE JOURNAL OF PHYSICAL CHEMISTRY A · JUNE 2011

Impact Factor: 2.69 · DOI: 10.1021/jp2050367 · Source: PubMed

---

CITATIONS

15

READS

31

## 5 AUTHORS, INCLUDING:



Jules Tshishimbi Muya

University of Richmond

19 PUBLICATIONS 164 CITATIONS

[SEE PROFILE](#)



Paul Geerlings

Vrije Universiteit Brussel

460 PUBLICATIONS 11,512 CITATIONS

[SEE PROFILE](#)



Minh Tho Nguyen

University of Leuven

748 PUBLICATIONS 10,835 CITATIONS

[SEE PROFILE](#)



Arnout Ceulemans

University of Leuven

252 PUBLICATIONS 4,094 CITATIONS

[SEE PROFILE](#)

# Theoretical Study on the Regioselectivity of the $B_{80}$ Buckyball in Electrophilic and Nucleophilic Reactions Using DFT-Based Reactivity Indices

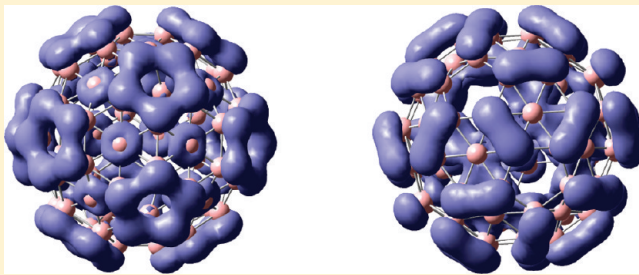
Jules Tshishimbi Muya,<sup>†</sup> Frank De Proft,<sup>‡</sup> Paul Geerlings,<sup>‡</sup> Minh Tho Nguyen,<sup>†</sup> and Arnout Ceulemans<sup>\*,†</sup>

<sup>†</sup>Department of Chemistry, and Mathematical Modeling and Computational Science Center (LMCC), Katholieke Universiteit Leuven, Celestijnenlaan 200F, B-3001 Leuven, Belgium

<sup>‡</sup>Eenheid Algemene Chemie (ALGC), Vrije Universiteit Brussel, Pleinlaan 2, B-1050 Brussels, Belgium

 Supporting Information

**ABSTRACT:** Density functional theory calculations at the B3LYP/SVP and B3LYP/6-311G(d) levels were carried out for a series of  $XH_3B_{80}$  complexes with  $X = \{N, P, As, B, Al\}$ . To probe the regioselectivity of  $B_{80}$ , the electronic Fukui function, the molecular electrostatic potential (MEP), and the natural bond orbital (NBO) were determined. These indices were shown to provide reliable guides to predict the relative reactivities of the boron buckyball sites. Thermodynamic stabilities of the complexes formed by the reaction of  $B_{80}$  with nucleophiles ( $NH_3, PH_3, AsH_3$ ) and electrophiles ( $BH_3, AlH_3$ ) are in good agreement with the prediction of regioselectivity indicated on the basis of Fukui and MEP indices. The qualitative results suggest the boron buckyball to be an amphoteric and hard molecule. It has two distinct reactive sites localized on caps and frame, which act as acids and bases, respectively. Most of the complexes are stable with formation energies comparable to that of the analogous complexes of the borane molecule,  $BH_3BH_3, BH_3NH_3$ , and  $BH_3AlH_3$ . The B—H—B bond characteristics of diborane are recovered in  $B_{80}BH_3$ . Exohedral complexes are more stable than endohedral complexes. The most stable complexes are those with  $NH_3$  on the caps and  $BH_3$  on the pentagonal ring of  $B_{80}$ .



## 1. INTRODUCTION

In contrast to carbon, the allotropes of elemental boron represent an unchartered territory. Few experimental studies are available, and exploration is largely carried out by theoretical and computational analyses. Having one electron less than its neighbor carbon, boron is electron deficient and must follow other strategies to form interboron covalent bonds. Theoretical studies show that this form of frustration may give rise to several astonishing architectures. In a recent article entitled “Boron Clusters Come of Age”, Grimes<sup>1</sup> argued that the variety of boron structures, such as neutral boranes, polyhedral boranes, and their derivatives, force us to rethink our concepts of covalent chemical bonding.

Polyhedral boranes have found many applications in medicine, pharmaceuticals, material sciences, and electronic industries.<sup>1,2</sup> As the electronic devices have reached the nanoscale, the boron nanomaterials are presumably interesting alternatives to carbon for future nanotechnologies. Jemmis et al.<sup>3</sup> compared carbon and boron chemistry and observed that in contrast with benzenoid aromatics systems in which condensation is based on edge-sharing, polyhedral boranes have several ways of condensing.

The study of bare boron clusters involves a systematic exploration of small cluster sizes, up to a few dozens of atoms, and the search for cluster expansion algorithms that would generate large hollow fullerene-like structures with hundred or more atoms. For the small clusters, experimental and theoretical evidence<sup>4</sup> has

been reported on planar boron clusters up to  $B_{15}$ . Further, it was shown that up to  $B_{19}$  clusters keep a planar geometry whereas  $B_{12}$  and  $B_{20}$  prefer double-ring tubular geometries.<sup>5,6</sup> The quasiplanarity of small boron clusters between  $B_{10}$  and  $B_{15}$  was also confirmed using photon electron spectroscopy.<sup>7</sup> It was found that the aromaticity effects favor circular shapes whereas the antiaromaticity promoted elongated forms.<sup>4,8</sup>

The interest in large spheroidal cages was initiated by the study of Szwacki et al.,<sup>8</sup> who claimed the existence of an extra stable closed-shell boron buckyball,  $B_{80}$ , with properties that would be reminiscent of the famous  $C_{60}$ , buckminsterfullerene.  $B_{80}$  consists of a 60-atom buckyball frame, made up of 12 pentagons, surrounded by rings of hexagons, but in addition every hexagon is capped by one extra boron, requiring thus 20 more boron atoms. Later on, alternative  $B_{80}$  structures were proposed, including core–shell clusters,<sup>9,10</sup> consisting of a  $B_{12}$  icosahedron, surrounded by a second shell of 68 boron atoms. Wang et al.<sup>11</sup> calculated a so-called volleyball shape, in which the pentagons are capped, and the remaining 8 caps are distributed over the hexagons, so as to yield a structure with  $T_h$  symmetry. This structure appears to be thermodynamically more stable than the

**Received:** May 30, 2011

**Revised:** June 30, 2011

**Published:** June 30, 2011

core–shell model  $B_{80}$  proposed by Zhao et al.<sup>10</sup> Of all these clusters, the original boron buckyball appears to have the largest HOMO–LUMO gap which suggests it to be kinetically more stable. This feature can be attributed to its leapfrog electronic structure.

In  $B_{80}$ , three types of boron are present, namely, the *endohe-dral* and *exohedral caps* in the center of the hexagons at a radial distance from the center which is smaller and larger, respectively, than the average radius of the cage, and the *frame* atoms located on the truncated icosahedral frame. Recently, Muya et al.<sup>12</sup> investigated the stability of encapsulated molecules of Group V atoms and revealed that  $B_{80}$  can stabilize unusual molecules such as tetrahedral  $P_4N_4$ , due to the acidity of the caps. Also, derivatives such as methyne boron buckyballs were anticipated to be stable, where boron caps are replaced by methyne groups, forcing carbon into a high coordination.<sup>13</sup> Clearly, a better understanding of the very special chemical properties of the different boron atoms is needed. In this paper, we aim to probe the special chemical microenvironment inside and outside of the buckyball, using well-established regioselective indicators for nucleophilic or electrophilic reactivities.

## 2. REGIOSELECTIVITY DESCRIPTORS

The reactivity of  $B_{80}$  is mainly characterized by Lewis acid–base reactions. Lewis defined a base as an entity that has at least one valence electron pair not involved in a covalent bond, and an acid as a species having at least one atom with a vacant orbital in which a pair of electrons can be accommodated.<sup>14</sup> The work of Fukui has indicated the important role of the frontier molecular orbitals, comprising the highest occupied molecular orbital (HOMO) and the lowest unoccupied orbital (LUMO), in the prediction of the reactions of organic compounds.<sup>15,16</sup> As boron chemistry is close to that of carbon, and the HOMO and LUMO of  $B_{80}$  are similar to that of  $C_{60}$ , the chemical properties of  $B_{80}$  can thus be understood by analyzing the frontier orbital structure. The introduction of density functional theory (DFT)<sup>17</sup> and the subsequent developments known as *conceptual DFT*<sup>17,18</sup> have further added to our understanding of concepts of chemical reactivity and generated additional quantitative measures to study reaction propensities.

The DFT method is based on the electron density function. The electron density is considered as the fundamental quantity for describing atomic and molecular ground states. Its response to the attack of a given reactant is expected to contain important chemical information. Consequently, reactivity indices have been introduced as response functions of the system energy with respect to either the number of electrons  $N$  of the system or its external potential  $\nu(\mathbf{r})$  (for an isolated system, this is just the potential due to the nuclei) or both.

The response of a system upon a perturbation of the electron density by the change of the number of its electrons, while the external potential of the system is kept constant, was introduced by Parr and Yang<sup>17</sup> as the electronic Fukui function.

$$\left( \frac{\partial \rho(\mathbf{r})}{\partial N} \right)_{\nu(\mathbf{r})} = f(\mathbf{r}) \quad (1.1)$$

The electronic Fukui function can be calculated by taking the difference in electron density between the ground state and the ion of a given molecule at the same external potential  $\nu(\mathbf{r})$ . Due to the  $N$ -discontinuity problem of atoms and

molecules, the left- and right-hand side derivatives at a given number of electrons correspond respectively to nucleophilic ( $f^+$ ), and electrophilic ( $f^-$ ) attack predictors.<sup>17–19</sup>

$$\left( \frac{\partial \rho(\mathbf{r})}{\partial N} \right)_{\nu(\mathbf{r})}^{\pm} = f^{\pm}(\mathbf{r}) \quad (1.2)$$

An approximation of the electronic Fukui function has been proposed which is described by a reduction of the function to HOMO and LUMO electron densities of the ground state corresponding to  $f^+$  and  $f^-$  descriptors.<sup>17,18</sup>

In view of the degeneracies occurring in the frontier molecular orbital energies of the systems investigated in this work,  $f^+$  and  $f^-$  were approximately computed as

$$f^+(\mathbf{r}) : \quad \frac{1}{D_{\text{LUMO}}} \sum_{i=1}^{D_{\text{LUMO}}} |\psi_{i,\text{LUMO}}(\mathbf{r})|^2 \quad (1.3)$$

$$f^-(\mathbf{r}) : \quad \frac{1}{D_{\text{HOMO}}} \sum_{i=1}^{D_{\text{HOMO}}} |\psi_{i,\text{HOMO}}(\mathbf{r})|^2 \quad (1.4)$$

$$\left( \frac{\partial \rho(\mathbf{r})}{\partial N} \right)_{\nu(\mathbf{r})}^{\pm} = f^{\pm}(\mathbf{r}) \quad (1.5)$$

as previously outlined.<sup>20</sup> In these equations,  $D_{\text{HOMO}}$  and  $D_{\text{LUMO}}$  correspond to the degeneracy of the LUMO and HOMO orbitals, respectively.

In view of the predominant role of the HOMO and LUMO densities in the Fukui functions, the success of the Fukui function in describing soft–soft interactions, as opposed to its failure in rationalizing hard–hard interactions is hardly surprising.<sup>21,22</sup> Note that Langenaeker et al.<sup>23</sup> argued that correlation effects are of minor importance.

The interaction between the electron density on the surface of the molecule with a given particular charge gives additional information on the chemical reactivity. The potential energy resulting from the interaction between a proton and the electron density distribution on the whole surface of a molecule is defined as the *molecular electrostatic potential*, denoted by MEP, and can be used to distinguish regions, which are poor or rich in electrons.<sup>24,25</sup> The MEP is a fundamental function in the determination of atomic and chemical properties as it directly depends on the electron density of the system. The expression of the MEP used in the present work is given by the following formula:<sup>24,25</sup>

$$V(\mathbf{r}) = \sum_A \frac{Z_A}{|R_A - \mathbf{r}|} - \int \frac{\rho(\mathbf{r}')}{|\mathbf{r}' - \mathbf{r}|} d\mathbf{r}' \quad (1.6)$$

$V(\mathbf{r})$  represents the electrostatic energy of a proton at given position  $\mathbf{r}$ . The summation over A describes the nuclear repulsion part;  $\rho(\mathbf{r}')$  stands for the electron density of the molecule and the integration represents the attraction exerted by the electronic cloud. It has been argued that the electrostatic potential should be used to probe the interaction of the system with hard electrophiles. In this work, we calculate both the electronic Fukui function and the molecular electrostatic potential to evaluate the probable reactive sites and their affinity toward hard and soft electrophiles and nucleophiles.

In view of the crucial role of the frontier orbitals in the acid–base reactivity, a useful complementary way of inspecting reactive sites in acid–base reactions is a detailed analysis of the

frontier molecular orbitals of  $B_{80}$ , which are expected to interact with the frontier molecular orbitals of the reactants. The natural bond orbital analysis (NBO)<sup>26</sup> may give additional support to the understanding of the chemical bonds (formation and breaking of bonds) in  $B_{80}$  on basis of the difference in hybridization of atomic orbitals on caps and frame. The complexes are formed when the HOMO of the nucleophile interacts with the LUMO of the electrophile.

### 3. COMPUTATIONAL METHODS

We have carried out DFT calculations using the hybrid functional B3LYP with the SVP basis set, as implemented in TURBOMOLE-V6.3 packages<sup>27,28</sup> to predict the equilibrium geometries of  $B_{80}$  complexes. All the stationary points were characterized by the default computational convergence criteria presented by the following threshold:  $10^{-7}$  for electronic energy change,  $10^{-3}$  for maximum coordinate displacement,  $10^{-4}$  for maximum gradient element, and  $5 \times 10^{-4}$  for rms of displacement and gradient. The nucleophiles considered in this work are the hydrides of Group V such as  $NH_3$ ,  $PH_3$ , and  $AsH_3$  and the electrophiles are  $BH_3$  and  $AlH_3$ . All these compounds have in common either a lone-pair p orbital or a vacant p orbital that can interact in acid–base reaction. The increase in size of these ligands allowed the influence of the softness (polarizability) in the complexation to be studied. For each ligand considered, six directions of approach to  $B_{80}$  were considered, which are indicated as endo-endo, endo-exo, exo-endo, exo-exo, endo-penta, and exo-penta. Endo-endo and endo-exo refer to a reactant which is encapsulated inside the cage (endohedral) and approaches the inward (endo-endo) or outward (endo-exo) pointing cap atoms. Exohedral adducts to the inward or outward pointing cap atoms are denoted as exo-endo and exo-exo, respectively. The exo-penta and endo-penta approaches are complexes between external and encapsulated ligands, respectively, and the frame borons. Hence, altogether with five ligands and six directions of approach, 30 combinations were examined. In view of this large number of optimized geometries, all in  $C_1$  symmetry, and taking into consideration the size of the molecules, we have run the frequency calculations at lower level B3LYP/STO-3G in order to have a qualitative idea whether these structures correspond to the minima on the potential energy surface.

The most stable complexes located at B3LYP/SVP were subsequently reoptimized at a higher level such B3LYP/6-311G-(d). The counterpoise correction<sup>29,30</sup> was computed to evaluate the basis set superposition error (BSSE).<sup>31</sup> Further, we have performed a reoptimization calculation including the dispersive energy of the low-lying  $B_{80}$ – $AsH_3$  complex using the density functional theory including dispersion corrections denoted as DFT-D<sup>32</sup> with B97-D functional<sup>33</sup> to analyze the influence of the dispersion energies in the stability of this complex.

The dispersion energies are generally associated with long-range bond distances, which in our study is the case for the arsine ligand. Previous studies on intermolecular interactions of a large benchmark set of biologically relevant molecules using density functional theory including dispersion corrections<sup>34</sup> concluded that the DFT-D model is very well suited for the description of the noncovalent interaction energies, and the B97-D functional was found to be more consistent functional in the description of nonconvalent complexes. According to their findings, the B3LYP-D does not provide better results compared to B97-D.

We have plotted the electronic Fukui function and the MEP as regioselectivity indexes. Gaussview,<sup>35</sup> gmolden,<sup>36</sup> and gOpenmol<sup>37</sup> suites of programs were used for visualization.

## 4. RESULTS

**4.1. Equilibrium Geometries of  $XH_3@B_{80}$  Complexes with  $X = \{N, P, As, B, Al\}$ .** The 2p valence shell of boron is filled by only one electron; the remaining p orbitals are vacant and ready to receive lone pair electrons. In  $B_{80}$ , the cap atoms transfer nearly three electrons to the frame,<sup>13</sup> and become more acid, while the electron population of the frame atoms increases slightly. The extent of the electron transfer from the caps is not sufficient to compensate the electron deficiency of the frame. As a result, the boron atoms in  $B_{80}$  behave as Lewis acids, which can receive lone pair electrons in their vacant p orbitals.

The group V hydride molecules  $NH_3$ ,  $PH_3$ , and  $AsH_3$  are electron-rich bases, having one lone pair of electrons to interact with  $B_{80}$ . An interesting regioselectivity arises because  $B_{80}$  contains different boron sites, caps and frame, and further in  $T_h$  symmetry. The cap atoms are divided into two groups, viz., the outward and inward caps, depending on the value of their radial distance to the center. We denote these caps as exo caps and endo caps. Moreover the ligands themselves can be located inside (endo- $B_{80}$ ) or outside the cage (exo- $B_{80}$ ), which further diversifies the reaction modes.

**Endohedral Complexes.** The optimized geometries computed at the B3LYP/SVP level with the ligands encapsulated in the cage and oriented on different sites of  $B_{80}$  are shown in Figure 1. Each of these complexes tells a story on its own, and we now discuss them one by one.

For  $NH_3$  the endo-endo or endo-exo directions of approach finally result in the same energy minimum, which is shown in Figure 1a. This shows the elasticity of the caps. When in the endo-exo mode  $NH_3$  approaches the exo-cap it pulls this cap inside, and in the same time seven other caps follow so as to return to the conformation with eight endo-caps forming a cube, and 12 exo-caps distributed in pairs over the faces of the cube.

For  $PH_3$  the situation is quite different. In the endo-endo mode,  $PH_3$  dissociates into  $PH_2 + H$ , and the heteroatom forms a bidentate bond to two neighboring caps, and the lone hydrogen atom is coordinated to a third cap (Figure 1b). These three caps are bent inward while the remaining caps are almost in the centers of the hexagons. This geometry coincides with the one in our earlier study on encapsulated molecules.<sup>12</sup> The endo-exo approach on the contrary yields a monodentate  $PH_3$ , with a cubic pattern of endo-caps as in the ammonia case (Figure 1c).

The bulkier encapsulated  $AsH_3$  keeps its compact geometry and gives rise to two isomers with the ligands occupying either a central (Figure 1d) or an off-center position (Figure 1e). The complex with  $AsH_3$  at the middle of the  $B_{80}$  cage is similar to the arsine encapsulated in buckyball complex reported in our earlier work.<sup>12</sup>

The acidic ligands  $BH_3$  (Figure 1f,g) and  $AlH_3$  (Figure 1h,i) tend to dissociate or to form multiple bonds in order to increase their stabilities. Like for  $PH_3$ , both  $BH_3$  and  $AlH_3$  complexes are of two types: for the endo-exo mode the ligand remains compact, while in endo-endo it dissociates into  $BH_2 + H$  and even  $Al + 3H$ . This certainly points toward a strong catalytic activity of the boron buckyball interior.

The geometric and energetic properties of these complexes are listed in Table 1. Complexes in which the guests conserve their compact shape with the heteroatom linked to one cap are less

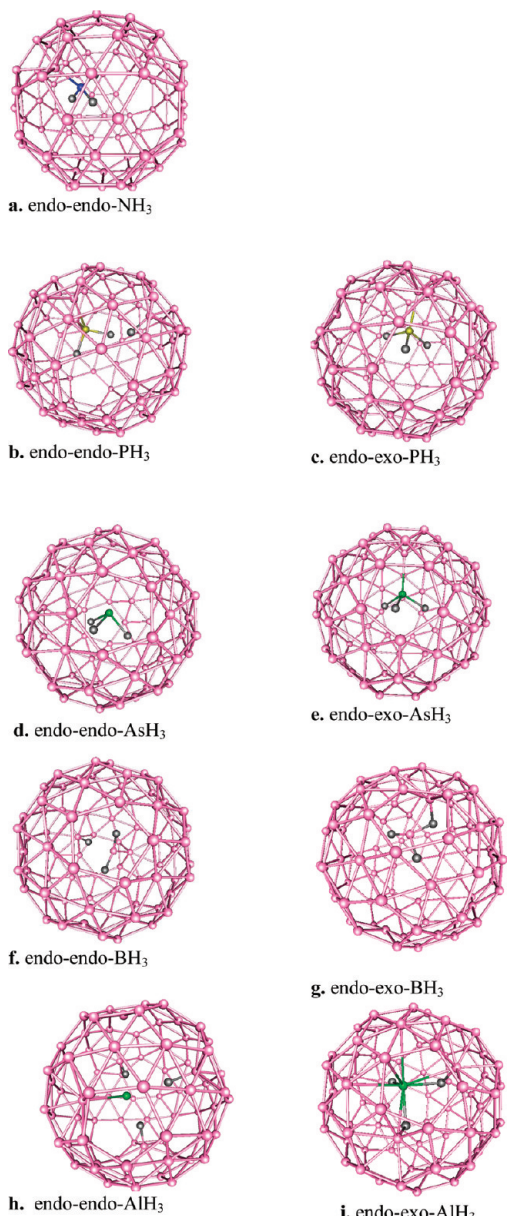


**Figure 1.** Optimized geometries of endohedral complexes  $\text{XH}_3@\text{B}_{80}$  at the B3LYP/SVP level.

stable compared to their homologues in which the encapsulated molecules are dissociated or the heteroatoms are linked to more neighboring boron atoms of the cage. For example, the endo-endo isomer of  $\text{PH}_3$  is 6.7 kcal/mol below the endo-exo- $\text{PH}_3$ . The dissociation of endo-endo- $\text{BH}_3$  into  $\text{BH}_2 + \text{H}$  fragments yields three extra bonds to the caps that lower the energy by 10.2 kcal/mol as compared to the endo-exo compact form. This compact  $\text{BH}_3$  encapsulated in  $\text{B}_{80}$  forms a kind of three-center  $\text{B}-\text{H}-\text{B}$  bond with bond geometry, which is very close to the  $\text{BH}_3\text{BH}_3$  bonds previously analyzed by Nguyen et al.<sup>38</sup> The  $\text{B}-\text{B}$  bonds between  $\text{BH}_3$  and the cap boron amount to 1.78 Å, the distances between the common hydrogen and  $\text{BH}_3$  and the cap are respectively 1.29 and 1.35 Å, and the two terminal  $\text{BH}$  bonds measure 1.19 Å (Figure 1g).

In general, the complexation energies of endohedral complexes decrease with the increasing size of molecules.  $\text{NH}_3$  forms

more stable complexes than  $\text{PH}_3$  or  $\text{AsH}_3$ . The ammonia and phosphine endohedral complexes are thermodynamically stable, whereas arsine endohedral complexes are metastable with complexation energies of 5.8 and 4.8 kcal/mol. This tendency of caps to react strongly with the hard base ammonia was also highlighted in our previous studies.<sup>12</sup> Nevertheless, the acidic  $\text{BH}_3$  and  $\text{AlH}_3$  molecules are also found to form with  $\text{B}_{80}$  thermodynamically exothermic endohedral complexes, albeit that these cases involve multiple bonding.

It should be noted that attempts to optimize complexes with  $\text{BH}_3$  and  $\text{NH}_3$  linked to the boron atoms on the frame did not yield stable endo-penta- $\text{XH}_3$  structures. The heteroatoms are repelled by the frame, and always prefer bonds with the caps as illustrated in the Figure 1 for  $\text{BH}_3$  and  $\text{NH}_3$ . Frame boron atoms are thus favorable for endohedral attack. The hybridization of the boron atomic orbitals on the pentagonal rings reflecting the effect of the curvature of  $\text{B}_{80}$  surface and the resilience of the buckyball frame to relax toward the heteroatom may be responsible for the instability of the endo-penta- $\text{XH}_3$  complexes. The influence of the curvature in the chemical reactivity was also pointed out in carbon fullerenes elsewhere.<sup>39</sup> In the next section we confront this finding with the reactivity indices.

**Exohedral Complexes.**  $\text{B}_{80}$  can also interact with molecules that are approaching from the outside of the cage. We have considered separately exohedral attacks on caps and on pentagonal sites. The complexes obtained were denoted as exo-exo- $\text{XH}_3$  and exo-endo- $\text{XH}_3$  for the reaction directed to the exo- and endo caps, respectively, and exo-penta- $\text{XH}_3$  for the complexes obtained by directing the ligand to the pentagonal rings. The optimized geometry of penta-exo- $\text{AsH}_3$  was computed at the B3LYP/6-311G(d) level.

The optimized geometries of exohedral complexes are given in Figure 2. The reaction modes for exohedral attack are less diverse, as compared to the endohedral ones. For reactions with the caps, all ligands are seen to keep their compact geometries. For nucleophilic ligands approaching the cap atoms, the initial orientation of the attacking nucleophiles toward exo or endo caps has no influence on the final geometry: for both orientations the coordinating cap is moving outward, again indicating the elasticity of the caps. Surprisingly, in these structures, 10 caps are moving inside the cage and 10 remaining antipodal ones are almost in a planar configuration. These complexes are characterized by bond distances between heteroatoms N, P, and As of  $\text{XH}_3$  ligands with the cap boron of 1.62 Å for  $\text{B}-\text{N}$ , 1.91 Å for  $\text{B}-\text{P}$ , and 1.90 Å for  $\text{B}-\text{As}$ . The HOMO–LUMO gaps of exo- $\text{XH}_3$  complexes are close to 1.90 eV, and cohesive energies amount to -28.8, -7.9, and -0.6 kcal/mol, for  $\text{NH}_3$ ,  $\text{PH}_3$ , and  $\text{AsH}_3$  complexes, respectively. Thus, the relaxation of the cage removes any regioselectivity between endo and exo caps. The endo cap attached to the ligand is pulled outward to form an exo cap and concomitantly the remaining caps relaxed also, yielding an equal partition of exo and endo caps.

The optimized geometries of exo-endo- $\text{XH}_3$  are identical to exo-exo- $\text{XH}_3$ . In contrast to endohedral complexes, the endo caps do not form any cube. Further, the HOMO–LUMO gaps in both endohedral and exohedral complexes formed by nucleophiles are very close to each other. Comparing the HOMO–LUMO gaps, and the complexation energies between monodentate endohedral and exohedral complexes of  $\text{NH}_3$ ,  $\text{PH}_3$  and  $\text{AsH}_3$  with  $\text{B}_{80}$ , it is seen that the nucleophilic exohedral complexes are more stable than the nucleophilic endohedral complexes reacting on the caps (Table 1). This can be explained by the steric hindrance exerted

**Table 1.** Formation Energies (FE) (kcal/mol), HOMO–LUMO Gaps (H-L) (eV), B–X (X = N, P, As, B, As) Bond Distances (Å), Total Energies ( $E_{\text{tot}}$ ) (au) at B3LYP/SVP<sup>a</sup>

ligands	endo-endo	endo-exo	exo-exo	exo frame	parameters
NH <sub>3</sub>	−2041.19239		−2041.19511	−2041.17689	$E_{\text{tot}}$
	−27.09		−28.8	−17.36	FE
	1.82		1.89	1.68	H-L
	1.61		1.62	1.64	B-N
	140		99	115	LF
PH <sub>3</sub>	−2327.68074	−2327.6701	−2327.67537	−2327.66371	$E_{\text{tot}}$
	−11.21	−4.54	−7.84	−0.53	FE
	0.7	1.85	1.91	1.65	H-L
	1.98–2.05	1.97	1.98	1.97	B-P
		153	94	78.76	LF
AsH <sub>3</sub>	−4221.95541	−4221.95702	−4221.96549		$E_{\text{tot}}$
	5.83	4.82	−0.5		FE
	1.97	1.87	1.9		H-L
	3.25	2.14	2.13		B-As
	82	93	69		LF
BH <sub>3</sub>	−2011.22859	−2011.26311		−2011.29391	$E_{\text{tot}}$
	5.74	−15.92		−35.25	FE
	1.8	1.72		1.86	H-L
	1.78	6.41		1.91–1.75	B-B
AlH <sub>3</sub>	−2228.79607	−2228.79693		−2228.81358	$E_{\text{tot}}$
	−22.78	−23.32		−33.77	FE
	1.92	0.71		1.82	H-L
	2.31–2.53	2.37		2.45–2.14	B-Al

<sup>a</sup> LF is frequency of the lowest vibrational mode (in cm<sup>−1</sup>).

by the cage on the encapsulated ligands. It is also confirmed by the slight shortening of B–X bond distances in endohedral complexes compared to exohedral complexes.

On the other hand, interactions between the electrophilic ligands, BH<sub>3</sub> and AlH<sub>3</sub>, and the caps are found to be repulsive. When the BH<sub>3</sub> or AlH<sub>3</sub> are placed at bond distances to the B<sub>80</sub> caps, they are repelled, as shown in Figure 2c for exo-exo-AlH<sub>3</sub>. Apparently, the caps, which are electron deficient, exert Coulombic repulsive interactions with the electrophilic ligands, since the heteroatoms of the latter carry partial positive charges.

For attack on the frame atoms, the pattern is quite different. Generally speaking, nucleophiles form weaker bonds and prefer monodentate coordination, while electrophiles form stronger bonds and prefer edge-on coordination. The nucleophiles attached on the frame of the B<sub>80</sub> complexes in exo-penta-NH<sub>3</sub>, exo-penta-PH<sub>3</sub>, and exo-penta-AsH<sub>3</sub> keep their compact shapes (Figure 2d–f). These complexes are less stable as compared to those formed by caps atoms on basis of their cohesive energies, and the HOMO–LUMO gap is less pronounced as shown in Table 1.

In contrast, electrophiles form highly stable complexes with pentagonal boron atoms. Both B<sub>80</sub>BH<sub>3</sub> and B<sub>80</sub>AlH<sub>3</sub> (Figure 2g,h) show substantial complexation energies of −35.3 and −33.8 kcal/mol, and appreciable HOMO–LUMO gaps of 1.86 and 1.82 eV, respectively. It is worth to note that these exo-penta-BH<sub>3</sub> and

exo-penta-AlH<sub>3</sub> complexes are only slightly less stable than diborane and alane–borane, about 7 and 1 kcal/mol, respectively. The stabilities of all complexes studied in the present work can also be discussed on the basis of their HOMO–LUMO gaps referring to the maximum hardness principle.<sup>40</sup>

Furthermore, adduct formation of BH<sub>3</sub> to the cage gives rise to two B–B bonds of 1.91 and 1.75 Å, and one B–H bond of 1.30 Å, as illustrated in Figure 3. These values are close to the B–B and B–H bonds in BH<sub>3</sub>BH<sub>3</sub> computed at the MP2/aug-cc-pVQZ level,<sup>37</sup> and similar bonds in BH<sub>3</sub>BH<sub>3</sub>BH<sub>3</sub>, NH<sub>3</sub>BH<sub>2</sub>BH<sub>2</sub>BH<sub>3</sub> calculated at MP2/aug-cc-pVTZ.<sup>41</sup> The AlH<sub>3</sub> adduct forms also a triangular ring with the cage with Al–H, of 1.58 Å, B–H bond of 1.25 Å, B–Al of 2.45 Å, and B–B bonds of 1.83 Å approaching the geometrical parameters of AlH<sub>3</sub>BH<sub>2</sub>NH<sub>3</sub>.<sup>42</sup>

The fact that the more polarizable AlH<sub>3</sub> is less bonding than BH<sub>3</sub> means that the boron atoms localized on the frame are hard and prefer hard Lewis acids to soft acids. In these complexes, BH<sub>3</sub> keeps its compact shape whereas the AlH<sub>3</sub> dissociates into AlH<sub>2</sub> + H. The BH<sub>3</sub> and AlH<sub>2</sub> groups form an edge-on triangle with the edge adjacent to two hexagons (Figure 3a,b). This bonding mode is in line with the observations in the endohedral complexes, where boron and aluminum also prefer bidentate bonds. The cyclization of these electrophilic molecules on the buckyball surface is reminiscent of cyclization reactions observed in carbon chemistry.

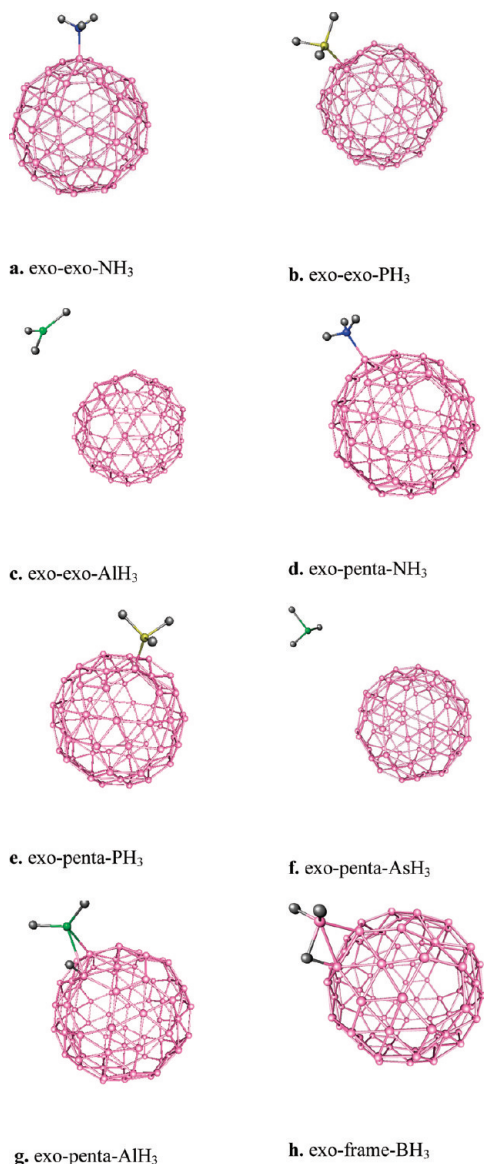


**Figure 2.** Optimized geometries of exohedral complexes  $\text{XH}_3@\text{B}_{80}$  at the B3LYP/SVP level.

**4.2. Reactivity Indices. Fukui Function Index.** Figure 4 depicts the Fukui functions for a nucleophilic (Figure 4a) and electrophilic (Figure 4b) attacks, respectively, of a soft reagent evaluated under icosahedral symmetry constraints. The influence of the small radial displacement of the capping atoms, which reduces the actual symmetry from  $I_h$  to  $T_h$ ,<sup>43</sup> is assumed to be negligible.

The Fukui function  $f^+$  plot (Figure 4a) shows the contribution of the caps, at either side of the spherical surface, while the frame borons localized on the pentagonal rings contribute only to the positive Fukui function via an exohedral component. Figure 4b depicts a reverse participation of caps and frame. In this map, the frame boron atoms contribute both inward and outward, whereas the caps participate only on the inside, but not exohedrally (Figure 5a,b, and Figure S1a–c in the Supporting Information).

In line with these findings, we can predict the outcome of acid–base reactions involving  $\text{B}_{80}$  and donor or acceptor molecules. The caps are acceptor sites in both endohedral and exohedral orientations. The frame atoms are acceptors only in

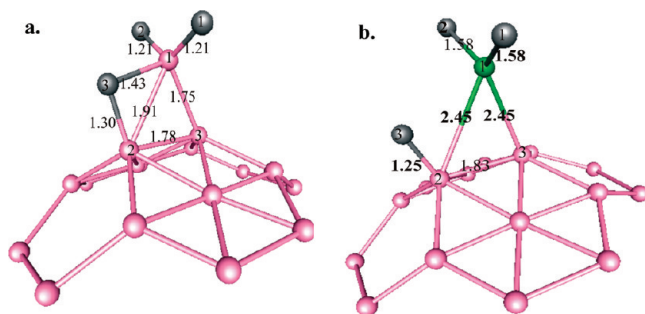


**Figure 3.** A view of cyclization of  $\text{BH}_3$  (a) and  $\text{AlH}_3$  (b) in exo-penta- $\text{BH}_3$  and exo-penta- $\text{AlH}_3$  complexes.

exohedral reactions. Consequently, stable acceptor–donor complexes can be obtained with some donors like  $\text{NH}_3$ ,  $\text{PH}_3$ , and  $\text{AsH}_3$  inside or outside the cage toward the caps and only outside the cage to the frame. Further, the frame can undergo both endohedral and exohedral chemical reactions with acceptor molecules such as  $\text{BH}_3$  or  $\text{AlH}_3$ . The cap atoms can interact only with acceptor molecules encapsulated in the cage. These predictions are corroborated by the results in Table 1. For instance, the electrophiles  $\text{BH}_3$  and  $\text{AlH}_3$  react strongly on the frame, but are repelled when they approach the caps from the outside.

When encapsulated,  $\text{BH}_3$  and  $\text{AlH}_3$  form exothermic complexes with the heteroatom attached to caps, but it should be noted that, in this case,  $\text{BH}_3$  and  $\text{AlH}_3$  decompose inside the cage in order to increase the stability of the complexes. The instability of endohedral complexes of  $\text{BH}_3$  in the endo-penta mode, illustrated by the spontaneous migration to caps is not in line with the predictions of the Fukui function  $f^-$ , and can be justified by the hybridization of atomic orbitals, the local curvature of the boron buckyball surface and the resilience of the frame boron to relaxation.

**Molecular Electrostatic Potential.** The reactivity of  $\text{B}_{80}$  toward hard electrophiles can be probed using the MEP, measuring the potential energy of a positive unit charge like a proton located at a particular distance near a molecule. A positive MEP region can be interpreted as a region where electrons are depleted, whereas a negative region shows the area where there is accumulation of electrons. The MEP of  $\text{B}_{80}$  depicted in Figure 6 was calculated at the B3LYP/SVP-optimized geometry.

The negative regions in green correspond to the attraction of the proton by the concentrated electron density in the molecule. It is related to the electrophilic reactions. The positive regions in red describe the repulsion of the proton, which corresponds to a favorable direction for nucleophilic attack. The pentagonal ring is rich in electrons and the center of hexagon is poor in electrons. Thus, capping atoms localized on the center of hexagons and those on the truncated icosahedron frame should repel electron-rich systems and attract electron-poor systems. This clearly confirms our finding that the boron atoms on the cap and frame orbits react differently. The caps are the best sites for nucleophilic attacks and the frame is the preferred site for electrophilic reactions with hard molecules. The frame atoms display higher basicity and nucleophilicity than the cap atoms, which are more acidic and electrophilic. Note that nucleophilicity and electrophilicity characterize kinetics whereas basicity and acidity describe the thermodynamics of interactions.

All sites in internal cage are highly deficient in electrons (Figure S2 in the Supporting Information); therefore, pentagonal rings and caps inside the cage are favorable for nucleophilic

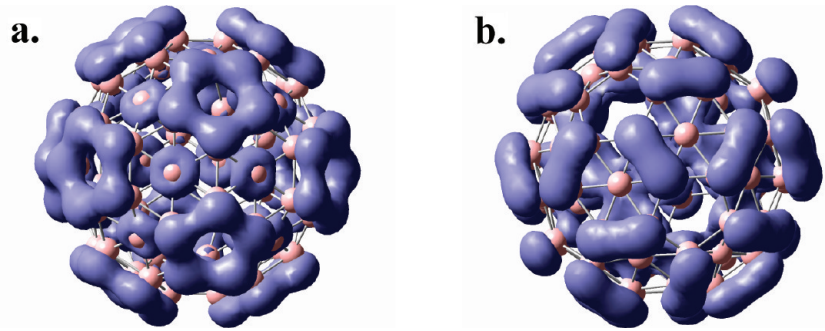


**Figure 4.** Electronic Fukui function: (a)  $f^+$  and (b)  $f^-$  of  $B_{80}$  in  $I_h$  symmetry (isocontours: 0.0016 au).

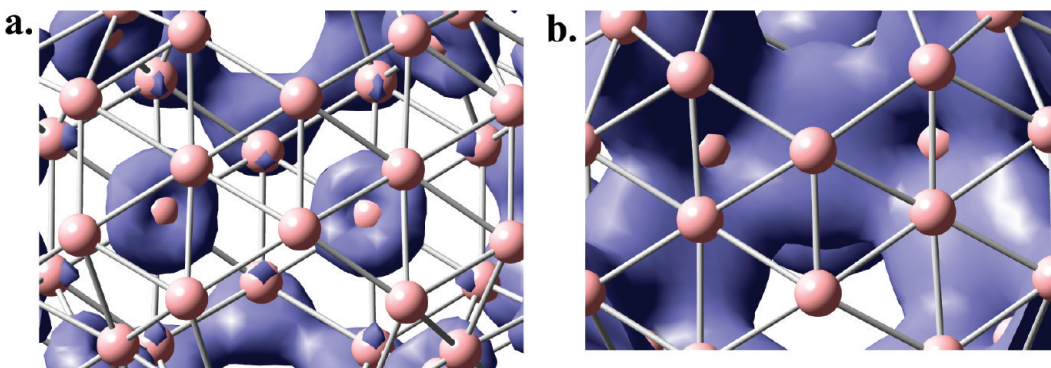


**Figure 5.** Internal detailed view of the electronic Fukui function; (a)  $f^-$  and (b)  $f^+$  of  $B_{80}$  in  $I_h$  symmetry (isocontours: 0.0016 au).

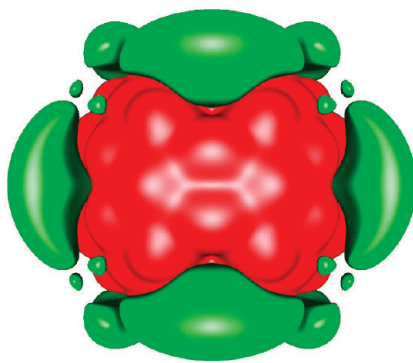


**Figure 6.** MEP of  $B_{80}$ . Positive regions are given in red (low electron density) and negative regions in green (high electron density) (isocontours:  $\pm 0.03$  au).

reactions rather than electrophilic reactions. The molecular electrostatic potential was used in the regioselectivity study of  $C_{60}$ ,  $C_{70}$ , and  $C_{76}$  fullerenes toward nucleophiles. It was claimed to be a reliable reactivity descriptor for systems when only changes of the geometrical parameters (increasing reactivity upon increasing curvature) were considered.<sup>39</sup> Chemical study of the stability of exohedral metallofullerenes revealed that the fullerenes react like polyalkenes and the metal atom preferred to attach to the 6–6 bond between hexagons.<sup>44</sup>

**Frontier Molecular Orbital Theory and Natural Bond Orbitals Analysis.** The  $B_{80}$  molecule has HOMOs and LUMOs of  $\pi$  character,<sup>43</sup> which belong to  $t_u$  symmetry (Figures 6).

**Table 2. Composition of Frontier Molecular Orbitals of  $B_{80}$  (B3LYP/SVP)**

FMOs and AOs	cap boron	frame boron
HOMO	0.15	1.61
S	0.00	0.69
$p_\sigma$	0.00	0.31
$p_\pi$	0.15	0.61
LUMO	0.50	1.50
S	0.09	0.93
$p_\sigma$	0.03	0.20
$p_\pi$	0.38	0.37

The HOMO is more localized on the frame with higher contribution of radial atomic orbitals whereas the LUMO contains a minor contribution of the cap atoms and a major contribution of frame atoms.

The cap orbitals in the LUMO are characterized by a nonnegligible participation of tangential  $p_\pi$  atomic orbitals (Table 2). A group-theoretical analysis predicts that in icosahedral symmetry there should be no contribution of radial  $p_\sigma$  orbitals on the caps in the HOMO as is confirmed in Table 2.

$BH_3$  and  $AlH_3$  Lewis acids exhibit vacant p orbitals. These p orbitals can react with radial atomic orbitals of electron-rich boron sites to form sigma bonds. The best candidate atomic orbitals on the spherical molecule are hybrid orbitals of s and  $p_\sigma$  character on the frame. We thus have to look at the HOMO of the buckyball (Figure 7a) to look for favorable interactions with the LUMO of the electrophile (Figure 7d). Clearly, the frame atoms are the only sites that are available for such interactions. The combination of

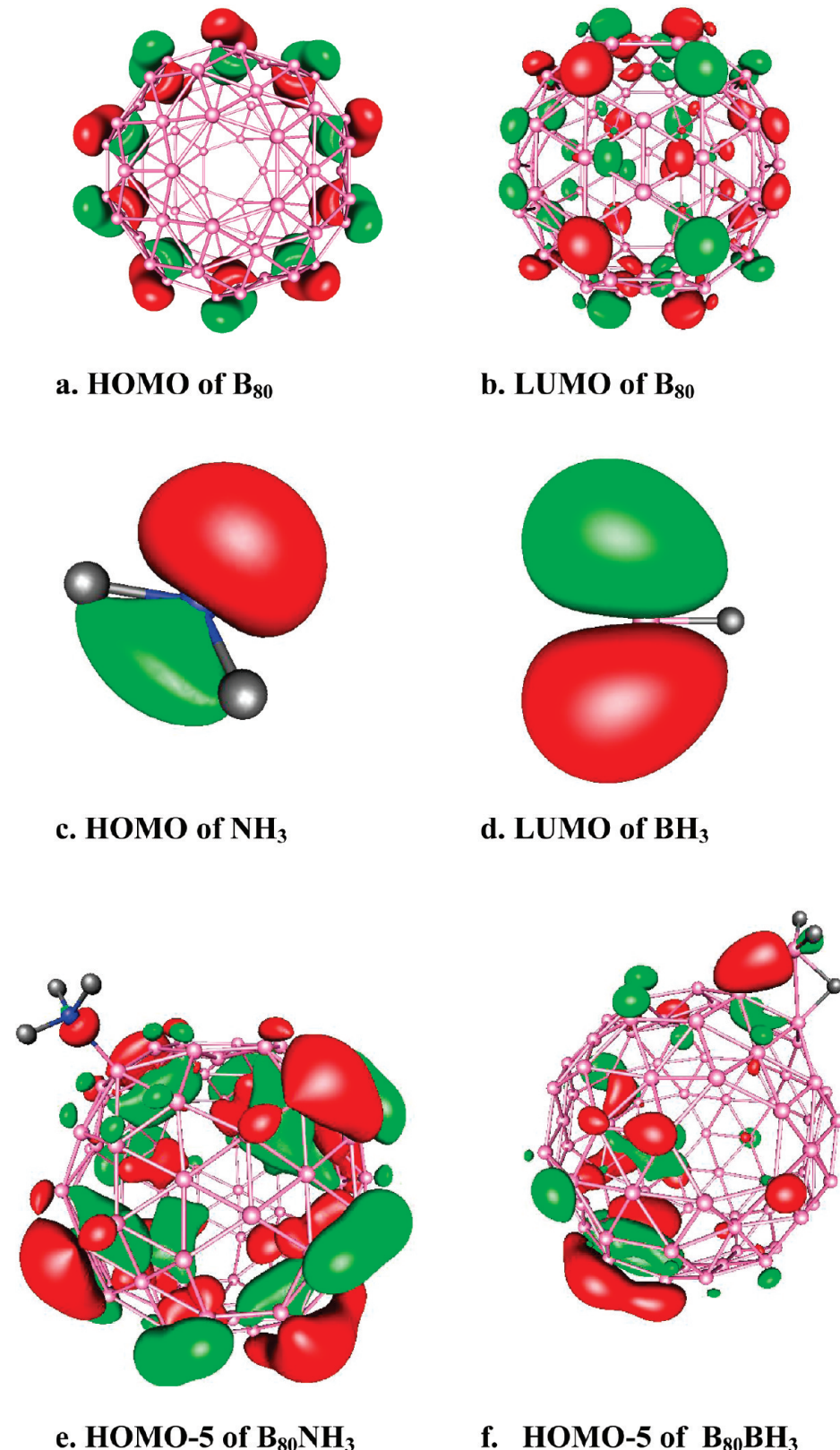


Figure 7. Frontier molecular orbitals of  $NH_3$ ,  $BH_3$ ,  $B_{80}$ , exo-exo- $NH_3$ , and exo-penta- $BH_3$ .

the HOMO and LUMO of the reaction partners gives a bonding molecular orbital, which is stabilized in energy. This corresponds to the HOMO-5 of the complex, as is shown in Figure 7f.

The curvature of the boron fullerene surface is correlated to the hybridization of atomic orbitals on different boron buckyball sites. We have quantified this curvature in terms of the pyramidal

Table 3. Wiberg Bond Order Index (Wi) of B<sub>80</sub>

B–B bonds	Wi	
	<i>I<sub>h</sub></i>	<i>T<sub>h</sub></i>
B <sub>1</sub> –B <sub>4</sub>	0.55	0.57
B <sub>1</sub> –B <sub>3</sub>	0.55	0.55
B <sub>1</sub> –B <sub>2</sub>	0.55	0.55
B <sub>4</sub> –B <sub>3</sub>	0.63	0.60
B <sub>2</sub> –B <sub>3</sub>	0.89	0.82
B <sub>4</sub> –B <sub>4</sub>	0.89	0.87
B <sub>2</sub> –B <sub>2</sub>	0.63	0.60

angle formed between the radial direction on a given site and the bonds with the adjacent atoms. This yields curvature angles of 91.2, 81.8, and 101.6°, for exo, endo, and frame sites, respectively. The pentagonal ring shows the higher value of the local curvature on the fullerene surface. A significant influence of the curvature and topology of carbon fullerenes surface in chemical reactivities was highlighted in ref 45. The reactivities of carbon fullerenes toward nucleophiles were found increasing with the increase of the curvature.<sup>39</sup> It is important to notice the plasticity character of caps in boron fullerenes which are able to change easily their local curvature under chemical reactions. The presence of caps makes the curvature of B<sub>80</sub> not uniform. The surface is composed of an alternation of positive and negative local curvatures. The outward motion of the caps breaks the folding of the surface and introduces local planar bonding regions of B<sub>4</sub> groups. This characteristic of boron fullerenes introduced by caps and their plasticity behavior is not present in carbon fullerenes.<sup>46</sup>

Baranov and co-workers<sup>47</sup> prepared the exohedral FeC<sub>60</sub><sup>+</sup> and concluded that this complex is dihapto-coordinated to a 6–6 double bond of the fullerene. According to Basir,<sup>48</sup> the preference of a pair of carbon atoms on 6–6 bonds against a single carbon interaction or a 6–5 bonds interaction (pentagon–hexagon) is due to the tilting of p orbitals in the icosahedron network away from the center caused by the curvature of the C<sub>60</sub> cage. In the same line, the p orbitals in the frontier orbitals of B<sub>80</sub> are also tilted from the center due to the curvature and can thus contribute to the preference of BH<sub>3</sub> and AlH<sub>3</sub> ligands to attach on the 6–6 bonds on the boron buckyball surface. Moreover, a linear correlation between heat effect of radical addition or polar compounds addition to fullerenes and local curvature indices of reaction sites have been reported, and this correlation expression was used in the prediction of reactivity of experimental results of C<sub>78</sub> in D<sub>3</sub> and C<sub>84</sub> in D<sub>2d</sub> toward H, F, and CH<sub>3</sub> radicals.<sup>49,50</sup>

We now consider the donor–acceptor orbital interaction for an incoming nucleophile, such as NH<sub>3</sub>. The lone-pair carrying HOMO of the ligand (Figures 7c) will seek interaction with the LUMO of the buckyball (Figures 7b). Boron is the least electronegative among the nonmetallic elements and it loses electrons when reacting with nitrogen, which is highly electronegative. This is illustrated by the polarization of the N–B bond as is illustrated in HOMO-5 of NH<sub>3</sub>–B<sub>80</sub> (Figure 7e) by a localization of an orbital lobe close to N along the B–N bond.

Because NH<sub>3</sub> and exo caps are hard, and the MEP on the hexagonal region is positive, the hard–hard interaction between NH<sub>3</sub> and B<sub>80</sub> is expected to be of dominant electrostatic character. The natural atomic occupancy and the natural electron configuration reveals a neat difference between cap and frame borons, with a valence electron configuration of 2s<sup>0.59</sup>2p<sup>2.44</sup> for

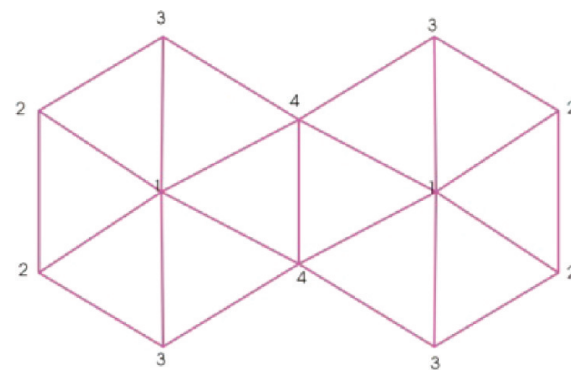


Figure 8. Double hexagon pattern.

the frame and 2s<sup>0.48</sup>2p<sup>2.45</sup> for the caps (the natural bond orbital analysis was carried out by using the NBO program at B3LYP/6-31G(d)).

The atomic orbitals of cap and frame form different hybrid functions, which can overlap to form chemical bonds. The B–B bonds on the pentagonal rings are formed by the linear combination of sp<sup>2.71</sup> hybrid functions and contain 1.52 or 1.56 electrons, leaving per atom one sp<sup>7.61</sup> nonbonding lone pair with 0.65 electrons. The cap boron atoms have one binding lone pair of p character having 0.89 electrons and three different nonbinding lone pair orbitals, of p, sp<sup>8.52</sup>, and sp<sup>0.12</sup> character, containing, respectively 0.89, 0.60, and 0.47 electrons.

The cap atoms tend to form a four-center bond with the common edge in between two adjacent hexagons, as previously mentioned.<sup>12,13</sup> Table 3 lists the bond order of the different B–B bonds in icosahedral B<sub>80</sub> carried out by NBO at B3LYP/6-31G(d) for an adjacent hexagons pattern with both caps exo for T<sub>h</sub> symmetry. The B<sub>1</sub> are atoms centered on hexagons and B<sub>3</sub>–B<sub>2</sub> bonds represent edges shared between two adjacent hexagons, as shown in Figure 8.

The bonds in between two hexagons are characterized by a Wiberg bond index order of 0.89 and 0.82 in I<sub>h</sub> and T<sub>h</sub>, respectively, and are likely approaching single covalent bonds. These are presumably preferential sites for electrophilic attacks. This suggestion is also supported by the topology of the optimized geometries of exo-penta-BH<sub>3</sub> and exo-penta-AlH<sub>3</sub> shown in Figure 3, where the edge-on coordination involves precisely the bond between hexagons, as opposed to the edge of a pentagon. The Wiberg bond index is much higher in C<sub>60</sub> and approach 1.61 and 1.39 for 5–6 and 6–6 bonds, respectively. The pentagonal ring is electron-deficient whereas the electron-rich bond is localized between hexagons.

## 5. DISCUSSION

The valence molecular orbitals of B<sub>80</sub> are similar to those of C<sub>60</sub>,<sup>13,43,51</sup> and boron fullerenes and carbon fullerenes are both electron-deficient systems. However, the chemical reactivity of B<sub>80</sub> is quite different from that of C<sub>60</sub>. While endohedral carbon fullerenes show only limited interactions with basic reactants forming weak chemical bonds, boron fullerenes interact strongly with hard compounds to form stable endohedral complexes.<sup>12</sup> Moreover, several specific addition modes are observed. The cyclization of acids BH<sub>3</sub> and AlH<sub>3</sub> on the bonds between two adjacent hexagons can be compared to cyclization reaction in Diels–Alder reactions on fullerenes. The comparison between

**Table 4.** Formation Energies (kcal/mol) and Bond Distances B–X (Å) of the Most Stable Stable Complexes for Different Complexes for  $B_{80}$  and  $BH_3^a$ 

adducts	orientation	B <sub>80</sub> complexes		borane complexes	
		formation energies	B–X bond	formation energies	B–X bond
H <sub>3</sub> N	cap exo-exo	−28.84	1.62	−35.82	1.65
H <sub>3</sub> P	cap endo-endo	−11.21	1.98; 2.05	−23.53	1.94
H <sub>3</sub> As	cap exo-exo	−0.55	2.13	−15.89	2.10
H <sub>3</sub> B	frame exo-penta	−35.25	1.75; 1.91	−40.64	1.79
H <sub>3</sub> Al	frame exo-penta	−33.77	2.14; 2.45	−35.03	2.19

<sup>a</sup> Computed at the B3LYP/SVP level with X = {N, P, As, B, Al}.

**Table 5.** Total Energies (TotE in hartrees), Basis Set Superposition Error (BSSE in hartrees), Formation Energies (FE in kcal/mol), and Bond Distances (B–X in Å) of the Most Stable Complexes for Different B<sub>80</sub> Adducts

adducts	orientation	TotE	BSSE	FE	B–X
H <sub>3</sub> N	exo-exo	−2044.41764	0.01071	−20.23	1.62
H <sub>3</sub> P	endo-endo	−2330.99142	0.00270	−9.95	1.96; 2.04
H <sub>3</sub> As	exo-exo	−4225.47617 (−4225.45938) <sup>a</sup>	0.00477	0.20 (−5.15)	2.13 (2.20)
H <sub>3</sub> B	exo-penta	−2014.47532	0.00306	−29.74	1.74; 1.91
H <sub>3</sub> Al	exo-penta	−2232.08420	0.00533	−28.49	2.13; 2.48

<sup>a</sup> Total energies calculated using DFT-D at B96-D/6-311G(d) of exo-exo-AsH<sub>3</sub> is given in parentheses and its associated formation energy is not corrected by BSSE.

the chemistry of boron fullerenes and carbon fullerenes could be inspiring to obtain a better understanding of boron chemistry, for which still many gaps remain.<sup>3</sup>

B<sub>80</sub> can also form specific internal cyclic bonds, as illustrated by the cyclic structures in endohedral B<sub>80</sub> complexes arising from the bidentate or multiple links of phosphorus, boron, and aluminum atoms in PH<sub>3</sub>–, BH<sub>3</sub>–, and AlH<sub>3</sub>–B<sub>80</sub> complexes (Figures 1 and 2). The total dissociation of AlH<sub>3</sub> and the partial dissociation of PH<sub>3</sub> and BH<sub>3</sub> molecules refer to a specific catalytic behavior of the hollow cage, which can be considered as a reactive microenvironment that can destabilize some strong chemical bonds. These results are also in agreement with previous findings that showed a partial dissociation of (CH<sub>3</sub>)<sub>2</sub>SH and PH<sub>3</sub> molecules encapsulated in boron buckyball.<sup>12</sup>

The complexation energies and bond distances between the heteroatom of the adducts and the boron atom of the B<sub>80</sub> cage for the most stable complexes such as NH<sub>3</sub>B<sub>80</sub>, BH<sub>3</sub>B<sub>80</sub>, and AlH<sub>3</sub>B<sub>80</sub> are approaching the formation energies and bond distances of small complexes such BH<sub>3</sub>NH<sub>3</sub>, AlH<sub>3</sub>BH<sub>3</sub>, and BH<sub>3</sub>BH<sub>3</sub> computed at the same level. Table 4 presents a comparison between BH<sub>3</sub> acid–base complexes and B<sub>80</sub> complexes with the same ligands. The results in Table 4 highlight once more that the cap atoms are more reactive toward nucleophiles, whereas the frame borons are more sensitive to electrophiles. Formation energies of the complexes point to an important role of polarizability and indicate that the B<sub>80</sub> prefers hard base/acid molecules to form more stable acid–base complexes. The favorable sites for electrophilic and nucleophilic additions, namely the frame sites for electrophiles and the cap sites for nucleophiles, agree with the predictions made by the Fukui functions, and MEP index. On the other hand, for the frame atoms, these indices do not really discriminate the outside and inside regions of the curved spherical surface, in contrast to the reaction modes that are clearly regioselective. Geerlings and collaborators<sup>39</sup> have investigated the relation between the reactivity of carbon fullerenes C<sub>60</sub>, C<sub>70</sub>, and C<sub>76</sub> toward nucleophiles and

studied the influence of the surface curvature. They found that the reactivity of these molecules was related to the geometrical constraints of the surface. The nucleophilic reactivity of these carbon fullerenes increased with the increase of the surface curvature. The molecular electrostatic potential predictions were in good agreement with the experimental data.

Regarding B<sub>80</sub>, the pentagonal ring is characterized by a higher local curvature and the surface effects clearly discriminate endohedral additions. On the other hand, the surface effect of addition on the caps is not so pronounced. This is entirely due to the plasticity of the caps, which is typical for the boron buckyball. The importance of this relaxation effect in the complexation reactions is illustrated in several ways. Complexation of ammonia to cap atoms at larger or shorter radial distance from the center leads to the same complexes, indicating the plasticity of the caps. On the other hand the absence of interactions with the frame atoms in the cage hollow indicates the rigidity of the frame itself. Finally, the higher stability of exohedral complexes to endohedral complexes may be due to the strain energy exerted by the cage.

Table 5 lists the formation energies corrected by BSSE, the total energies and the B–X bonds of the most stable complexes at the B3LYP/6-311G(d) level.

As expected, hard bases and hard acids, namely NH<sub>3</sub> and BH<sub>3</sub>, form with B<sub>80</sub> the most stable complexes, which confirm again that B<sub>80</sub> is a hard material. This result is in line with the molecular electrostatic potential map. The BSSE corrections do not change significantly the trend of stabilities among these acid–base complexes. The binding energies of the most stable complexes are approaching the binding energies of exohedral metallofullerenes MC<sub>60</sub><sup>+</sup> (with M = Mg, Fe, Mn, Cr, Mo, and W) lying in between 1 and 3 eV produced by means of ion beam scattering techniques.<sup>48</sup> The computed DFT-D of exo-exo-AsH<sub>3</sub> complex at the B96-D/6-311G(d) level yields a thermodynamically favorable formation energy. This suggests that the dispersion effects are important in AsH<sub>3</sub>B<sub>80</sub> complexes. However, this

value nearly  $-5.15$  kcal/mol is still small if we consider the basis set superposition error at the same B96-D/6-311G(d) level. The bond distance B—As in exo-exo-AsH<sub>3</sub> complex is 0.07 Å longer than that computed at B3LYP/6-311G(d).

## 6. CONCLUDING REMARKS

A theoretical study on the regioselectivity of boron buckyball B<sub>80</sub> confirms that the cap boron atoms are hard acids and the frame boron atoms are hard bases. Thus, B<sub>80</sub> appears as an amphoteric molecule containing acidic and basic sites. In agreement with this finding, the adducts of NH<sub>3</sub> and BH<sub>3</sub> are found to yield the most stable complexes and their binding energies are approaching that of ammonia borane and diborane. The frame can interact strongly with acids but only weakly with base molecules. The triangular rings formed by BH<sub>3</sub> and AlH<sub>3</sub> with the cage have geometries with B—B, and B—H bonds distances similar to BH<sub>3</sub>BH<sub>3</sub>BH<sub>3</sub> and AlH<sub>3</sub>BH<sub>3</sub> compounds. It is thus expected that B<sub>80</sub> will be able to retain on its surface BH<sub>3</sub> and AlH<sub>3</sub> molecules that could probably play a role of great interest for hydrogen storage. Caps are electron deficient and repel quite strongly exohedral electrophilic molecules. B<sub>80</sub> is also expected to be an important catalyst in acid–base reactions. The regioselectivity predictions made by the Fukui function and the MEP pictures are in agreement with the calculated formation energies of endohedral and exohedral acid–base complexes, but, in the case of the frame sites, are not sensitive to the effect of curvature.

## ■ ASSOCIATED CONTENT

**S Supporting Information.** Electronic Fukui function and molecular electrostatic potential of B<sub>80</sub> in I<sub>h</sub> symmetry and detailed views of their internal contributions. All atoms were expressly omitted for Fukui function. This material is available free of charge via the Internet at <http://pubs.acs.org>.

## ■ AUTHOR INFORMATION

### Corresponding Author

\*E-mail: arnout.ceulemans@chem.kuleuven.be.

## ■ ACKNOWLEDGMENT

The authors thank the Flemish Fund for Scientific Research (FWO-Vlaanderen) and Flemish Concerted Research Action (GOA) for continuing support. J.T.M. thanks the Arenberg doctoral school for a scholarship. F.D.P. and P.G. acknowledge the FWO-Vlaanderen and Free University of Brussels (VUB) for support.

## ■ REFERENCES

- (1) Grimes, R. N. *J. Chem. Educ.* **2004**, *81*, 657.
- (2) Sivaev, I. B.; Bregadze, V. V. *Eur. J. Inorg. Chem.* **2009**, *11*, 1433.
- (3) Jemmis, E. D.; Prasad, D. L. V. K. *Curr. Sci.* **2008**, *95*, 1277.
- (4) (a) Zhai, H.-J.; Kiran, B.; Li, J.; Wang, L.-S. *Nat. Mater.* **2003**, *2*, 827. (b) Nguyen, M. T.; Matus, M. H.; Ngan, V. T.; Grant, D. J.; Dixon, D. A. *J. Phys. Chem. A* **2009**, *113*, 4895. (c) Tai, T. B.; Grant, D. J.; Nguyen, M. T.; Dixon, D. A. *J. Phys. Chem. A* **2010**, *114*, 994.
- (5) (a) Alexandrova, A. N.; Boldyrev, A. I.; Zhai, H.-J.; Wang, L.-S. *Coord. Chem. Rev.* **2006**, *250*, 2811. (b) Kiran, B.; Bulusu, S.; Zhai, H.-J.; Yoo, S.; Zeng, X. C.; Wang, L.-S. *Proc. Natl. Acad. Sci.* **2005**, *102*, 963.
- (6) Kiran, B.; Gopakumar, G.; Nguyen, M. T.; Kandalam, A. K.; Jena, P. *Inorg. Chem.* **2009**, *48*, 9965.
- (7) Huang, W.; Sergeeva, A. P.; Zhai, H.-J.; Averkiev, B. B.; Wang, L.-S.; Boldyrev, A. I. *Nat. Chem.* **2010**, *1*, 534.
- (8) Szwacki, N. G.; Sadrzadeh, A.; Yakobson, B. I. *Phys. Rev. Lett.* **2007**, *98*, 165.
- (9) Li, H.; Shao, N.; Shang, B.; Yuan, L.-F.; Yang, J.; Zeng, X. C. *Chem. Commun.* **2010**, *46*, 3878.
- (10) Zhao, J.; Wang, L.; Li, F.; Chen, Z. *J. Phys. Chem. A* **2010**, *114*, 9969.
- (11) Wang, X.-Q. *Phys. Rev. B* **2010**, *82*, 153409.
- (12) Muya, J. T.; Lijnen, E.; Nguyen, M. T.; Ceulemans, A. *J. Phys. Chem. A* **2011**, *115*, 2268.
- (13) Muya, J. T.; Nguyen, M. T.; Ceulemans, A. *Chem. Phys. Lett.* **2009**, *483*, 101.
- (14) Pearson, R. G. *J. Chem. Educ.* **1968**, *45*, 581.
- (15) Fukui, K. *Angew. Chem.* **1982**, *21*, 801.
- (16) Fukui, K. *Pure Appl. Chem.* **1982**, *54*, 1825.
- (17) Parr, R. G.; Yang, W. *J. Am. Chem. Soc.* **1984**, *106*, 4049.
- (18) (a) Geerlings, P.; De Proft, F.; Langenaeker, W. *Chem. Rev.* **2003**, *103*, 1793. (b) Chandra, A. K.; Nguyen, M. T. *Chemical Concepts from Quantum Chemical Mechanics. Faraday Discuss.* **2007**, *135*, 191.
- (19) Zhang, Y.; Yang, W. *Theor. Chem. Acc.* **2000**, *103*, 346.
- (20) Flores-Moreno, R. *J. Chem. Theory Comput.* **2010**, *6*, 48.
- (21) Torrent-Sucarrat, M.; De Proft, F.; Geerlings, P.; Ayers, P. W. *Chem. Eur. J.* **2008**, *14*, 8652.
- (22) Chattaraj, P. K. *J. Phys. Chem. A* **2001**, *105*, 511.
- (23) Langenaeker, W.; De Proft, F.; Geerlings, P. *Chem. Phys. Lett.* **1996**, *256*, 400.
- (24) Bonaccorsi, R.; Scrocco, E.; Tomasi, J. *J. Chem. Phys.* **1970**, *52*, 5270.
- (25) Geerlings, P.; Langenaeker, W.; De Proft, F.; Baeten, A. *Theoretical and Computational Chemistry*, Murray, J. S., Sen, K. D., Eds.; Elsevier Science: New York, 1996; Vol. 3, p 587.
- (26) Foster, J. P.; Weinhold, F. *J. Chem. Phys.* **1983**, *78*, 4066.
- (27) Turbomole V6.3, a development of Universität Karlsruhe (TH) and Forschungszentrum Karlsruhe GmbH, 1989–2007, TURBOMOLE GmbH, since 2007.
- (28) Ahlrichs, R.; Bär, M.; Häser, M.; Horn, H.; Kölmel, C. *Chem. Phys. Lett.* **1989**, *162*, 165.
- (29) Boys, S. F.; Bernardi, F. *Mol. Phys.* **1970**, *19*, 553.
- (30) Van Duijneveldt, F. B.; Van Duijneveldt-Van de Rijdt, J. G. C. M.; Van Lenthe, J. H. *Chem. Rev.* **1994**, *94*, 1873.
- (31) Simon, S.; Duran, M.; Dannenberg, J. J. *J. Chem. Phys.* **1996**, *105*, 11024.
- (32) Grimme, S. *J. Comput. Chem.* **2004**, *25*, 1463.
- (33) Grimme, S. *J. Comput. Chem.* **2006**, *27*, 1787.
- (34) Antony, J.; Grimme, S. *Phys. Chem. Chem. Phys.* **2006**, *8*, 5287.
- (35) GaussView 4.1.2; Gaussian, Inc.; Wallingford, CT, 2004.
- (36) <http://www.cmbi.ru.nl/molden/>.
- (37) Laaksonen, L. *J. Mol. Graph.* **1992**, *10*, 33.
- (38) Nguyen, V. S.; Matus, M. H.; Nguyen, M. T.; Dixon, D. A. *J. Phys. Chem. A* **2008**, *112*, 9946.
- (39) Choho, K.; Langenaeker, W.; Van De Woude, G.; Geerlings, P. *J. Mol. Struct. (Theochim.)* **1994**, *338*, 293.
- (40) Chattaraj, P. K.; Lee, H.; Parr, R. G. *J. Am. Chem. Soc.* **1991**, *113*, 1855.
- (41) Nguyen, V. S.; Swinnen, S.; Nguyen, M. T. *Chem. Phys. Lett.* **2010**, *500*, 237.
- (42) Nguyen, V. S.; Matus, M. H.; Nguyen, V. T.; Dixon, D. A. *J. Phys. Chem. C* **2008**, *112*, 5662.
- (43) Gopakumar, G.; Nguyen, M. T.; Ceulemans, A. *Chem. Phys. Lett.* **2008**, *475*, 4540.
- (44) Śliwa, W. *Trans. Met. Chem.* **1996**, *21*, 583.
- (45) Zhou, C.; Wu, J.; Han, B.; Yao, S.; Cheng, H. *Phys. Rev. B* **2006**, *73*, 195324.
- (46) Muya, J. T.; Gopakumar, G.; Nguyen, M. T.; Ceulemans, A. *Phys. Chem. Chem. Phys.* **2011**, *13*, 7524.
- (47) Baranov, V.; Böhme, D. *Int. J. Mass Spectrom. Ion Processes* **1995**, *149/150*, 543.

- (48) Basir, Y. J.; Anderson, S. L. *Int. J. Mass Spectrom. Ion Processes* **1999**, *185/186/187*, 603.
- (49) Sabirov, D. Sh.; Bulgakov, R. G. *Comput. Theor. Chem.* **2011**, *963*, 185.
- (50) Sabirov, D. Sh.; Bulgakov, R. G.; Khursan, S. L. *Arkivoc* **2011**, *viii*, 200.
- (51) Ceulemans, A.; Muya, J. T.; Gopakumar, G.; Nguyen, M. T. *Chem. Phys. Lett.* **2008**, *461*, 226.